An Investigation of Electromagnetic Transient Characteristics on A Practical 500 kV Submarine Cable System

N. Jiang, C. Yang, H. Xue and J. Mahseredjian

Abstract--This paper performs an investigation on electromagnetic transients for a practical 500 kV cable system. The system consists of 500 kV overhead lines, submarine and underground cables. In order to study the insulation coordination of the cable system, the transient simulations are performed using EMTP. The modal propagation constants of submarine cable are also investigated. Moreover, the cable series and shunt parameters are calculated using the newly developed Line/Cable Data Module in EMTP. The voltage and current characteristics of the cable system in steady-state, and for switching, fault and lightning transients, are studied. The transient overvoltage levels are also compared with requirements of insulation coordination in local standards. The work shown in this paper could provide a reference for the insulation design of 500 kV cable system.

Keywords: Submarine cable, transmission system, series impedance, shunt admittance, propagation constant, transient voltage, EMT-type software

I. INTRODUCTION

THE implementation of submarine cables in offshore renewable energy and regional power interconnection is becoming more and more important. As a result, the mixed transmission system consisting of overhead lines, submarine and underground cables will be dominant in future power systems [1]-[5].

This paper performs a thorough investigation of transient voltages based on a practical 500 kV mixed transmission system with overhead lines, submarine and underground cables [6]. The major section of the transmission system is a 500 kV power cable. The system has been used to connect remote archipelago and offshore renewable energy to marine coast in south eastern part of China. It will further improve the strength of local power system and optimize the structure of network.

The above-mentioned mixed transmission system adopts the world's first 500 kV XLPE submarine cable [6]. The XLPE cable has several advantages i.e. large transmission capacity, high working temperature and environment friendly [1]. Since the overhead lines and buried cables have different electromagnetic parameters, it may produce more serious transient behavior due to reflections and refractions at various discontinuities [1]. Therefore, it requires detailed electromagnetic transient study to evaluate the withstand voltage of cables [1], [7], [8].

In general, the cable models for transient studies rely on series and shunt per-unit-length (pul) parameters [9]-[11]. Recently, a new Line/Cable Data (LCD) Module in EMTP [12]-[20] has been developed. The series and shunt parameters of cables can be calculated using new LCD with consideration of accurate earth-return, skin and proximity effects.

Considering the above facts, this paper introduces a systematical study of electromagnetic transient on submarine and underground cables in the 500 kV mixed transmission system. It should be noted that the new LCD is used to calculate cable series impedance and shunt admittance. In Section II, the configuration and parameters of the system are introduced and described. Section III focuses on investigations of responses on cable in frequency domain. The modal attenuation constant and phase velocity of cable are calculated.

In Section IV, steady-state, switching transient, short-circuit and lightning studies are performed on the mixed transmission system using EMTP [21] with its wideband (WB) line and cable models [22]. The core voltage and distribution of maximum transient voltage on sheath and armor are investigated with different conditions. The results discussed in this paper provide a reference for the insulation coordination of a 500 kV cable in the mixed transmission system.

II. DESCRIPTION OF POWER CABLE SYSTEM

A practical 500 kV submarine and underground cable system is shown in Fig. 1 [6], and the system consists of upper (red) and lower (black) circuits which include several parts, i.e. submarine and underground cables. Also, both ends of cables are connected to local 500 kV overhead lines. This mixed transmission system has been adopted to enhance power delivery between several large islands and marine coast in south eastern part of China.

The 500 kV power cable system has submarine and underground parts. The cross-section of a single-phase cable is illustrated in Fig. 2. The parameters of core, sheath and armor are given in Table I based on information and method used in reference [6]. Moreover, the wired conductors of armor and sheath can be modeled by new LCD, as explained in reference [6]. Each phase of submarine cable is buried into seabed with depth of 2.5 m. The phase separation of submarine part is 50 m.

N. Jiang, C. Yang and H. Xue are with GEIDCO, China (e-mails: nan-jiang@geidco.org, cheng-yang@geidco.org, haoyan-xue@geidco.org).
J. Mahseredjian is with Polytechnique Montréal, Canada (e-mails: jeanm@polymtl.ca).
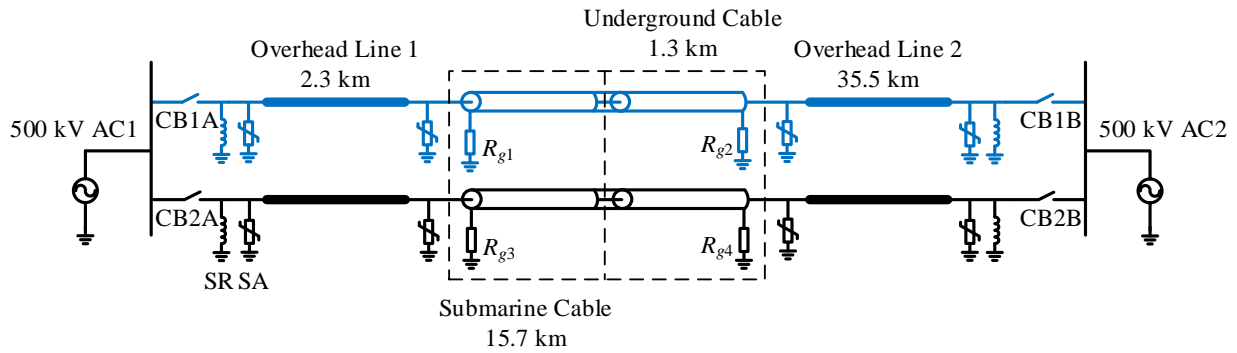
Fig. 1 A practical 500 kV submarine and underground cable system [6], blue: upper circuit, black: lower circuit.

Regarding underground part, it is the same as the submarine cable except that separation and buried depth are set to 7 m and 1.5 m respectively. It should be noted that mutual coupling between each phase of cable is only considered for underground section.
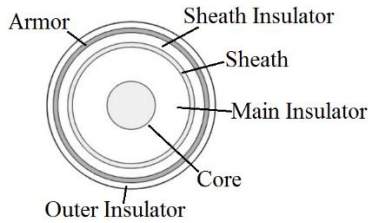
Fig. 2 Cross-sections of submarine and underground cables [6].

TABLE I
PARAMETERS OF SUBMARINE AND UNDERGROUND CABLE

	Radius (mm)		Resistivity (Ωm)
Core	Inner	Outer	2.83×10^{-8}
	0	25.75	
Main Insulator	Relative Permittivity ε_r		-
	2.74		
Sheath	Radius (mm)		Resistivity (Ωm)
	Inner	Outer	2.14×10^{-7}
	62.5	67.5	
Sheath Insulator	Relative Permittivity ε_r		-
	6.58		
Armor	Radius (mm)		Resistivity (Ωm)
	Inner	Outer	1.99×10^{-8}
	78	82.95	
Outer Insulator	Relative Permittivity ε_r		-
	2.2		
Outer Radius (mm)	89.5		

The configuration of the 500 kV overhead line (lines 1 and 2) is shown in Fig. 3. The radii of each phase and ground conductors are 1.465 and 0.64 cm, respectively. The DC resistances of phase and ground conductors are set to 0.0646 and 0.864 Ω/km. The bundle radius is 32.53 cm.

The earth resistivity is assumed to be 20 Ωm for both overhead lines and underground cables. The depth of seawater is assumed to be 15 m. The seawater and seabed resistivities are set to 0.2 Ωm and 20 Ωm respectively.
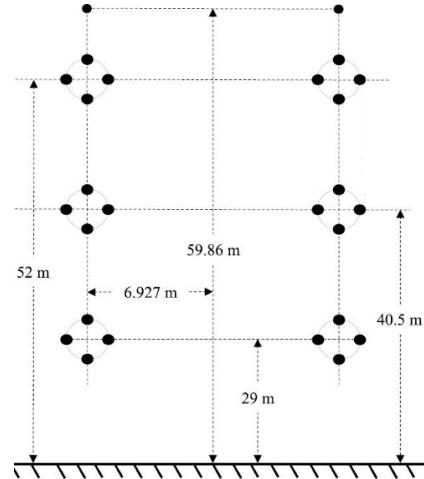
Fig. 3 Configuration of a 500 kV overhead line.

III. FREQUENCY RESPONSE STUDY

The frequency-dependent diagonal elements of 3-by-3 series impedance matrix are shown in Fig. 4.

The resistances R_{11}, R_{22} and R_{33} increase as frequency increases. The resistances in low frequency show significant differences due to variations of conductor resistivity. However, the inductances L_{11}, L_{22} and L_{33} decrease as frequency increases.

No instable characteristics are observed for the impedance calculation with consideration of seawater and seabed structure.

(a) Resistance

(b) Inductance
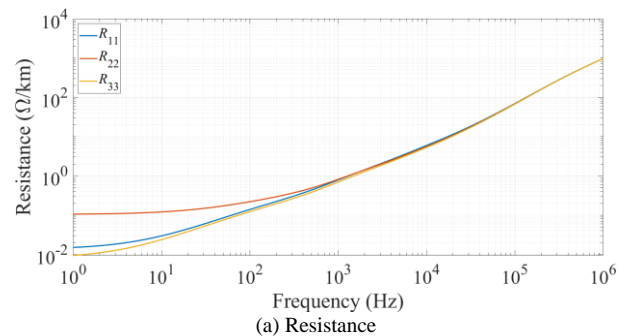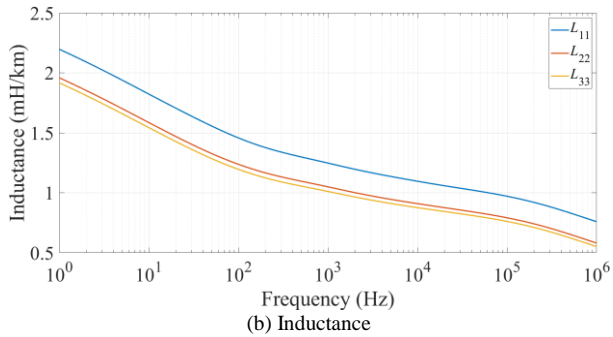
Fig. 4 Diagonal elements of series impedance matrix of cable shown in Fig. 2.

The modal propagation constants calculated using the cable shown in Fig. 2 are illustrated in Fig. 5. Since the cable only has 3 conductors, it has two co-axial and one earth-return propagation modes. It is clear that the modal attenuation constants increase as frequency increases. The modal phase velocities become stable above 1 kHz.

(a) Attenuation constant

(b) Phase velocity
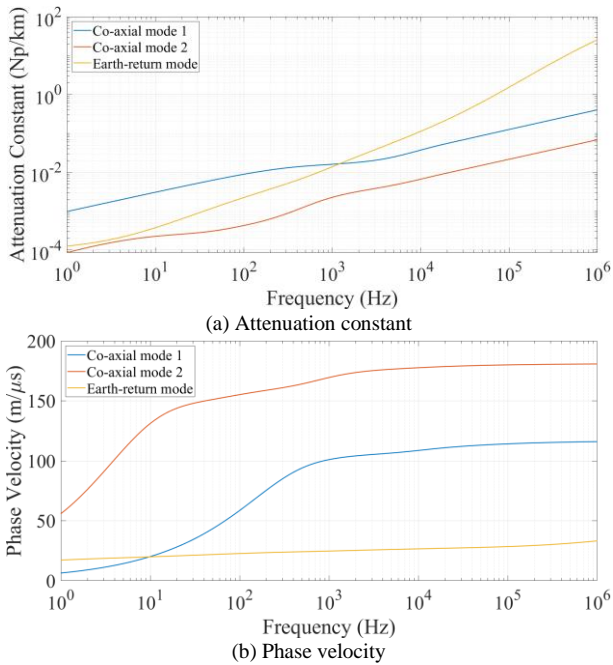
Fig. 5 Modal propagation constants of cable shown in Fig. 2.

IV. ELECTROMAGNETIC TRANSIENT STUDY

In this section, the cable system is simulated using an existing EMT-type simulation software. The voltage profiles and characteristics of the cable considering steady-state, energization, short-circuit and lightning conditions are investigated. The wideband model has been adopted into the following time domain simulations.

The sheath and armor of both submarine and underground cables are solidly bonded and grounded at both ends, as shown in Fig. 1. The grounding resistance R_g is set to 4 Ω for steady-state, energization and short-circuit studies. Regarding lightning transient, the resistance R_g is replaced by the following high frequency lumped grounding circuit [23].
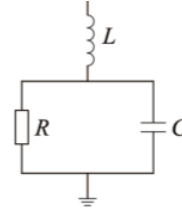
Fig. 6 High frequency lumped grounding circuit.

In Fig. 6, the parameters of lumped inductance L, resistance R and capacitance C are set to 5.27 μH, 4 Ω and 119 nF respectively, and those parameters are based on typical lightning transient grounding circuit in [23].

Furthermore, the surge arresters shown in Fig. 1 are modeled by ZnO device in the EMT-type simulation software.

A. Induced Voltage on Sheath and Armor in Steady State

Fig. 7 illustrates the induced voltages on sheath and armor of Phase A for cable in upper circuit during steady-state condition. The maximum sheath voltages at different positions of the cable are summarized in TABLE II.

It should be noted that the sending end of submarine cable and receiving end of the underground cable are located at 0 km and 17 km respectively. The discontinuity between submarine and underground cables appears at 15.7 km.
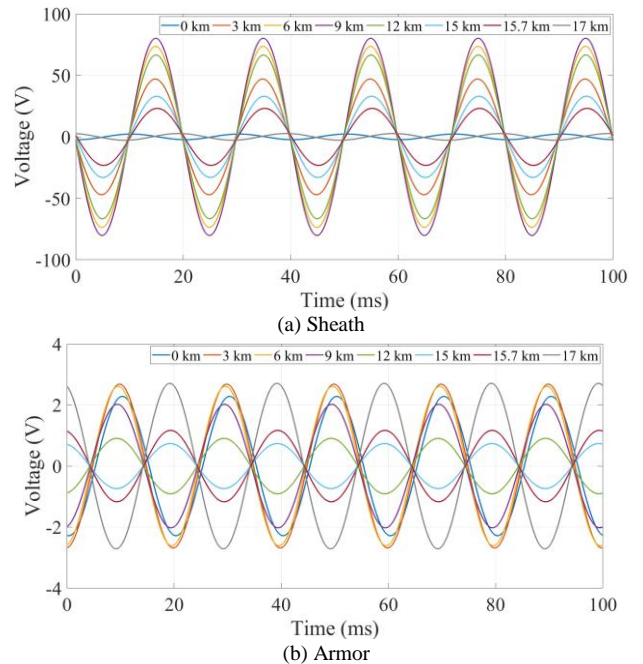
(a) Sheath

(b) Armor

Fig. 7 Induced voltages in steady-state on sheath and armor of cable in upper circuit, Phase A.

TABLE II
MAXIMUM SHEATH VOLTAGE OF CABLE IN UPPER CIRCUIT

Position (km)	0	3	6	9	12	15	15.7	17
Voltage (V)	2.2	47.1	73.6	80.1	66.6	33.2	23.1	2.6

It is clear that high voltage concentrates in the region between 6 km and 12 km. The maximum induced sheath voltage appears at 9 km and reaches 80.1 V. Furthermore, the induced voltages on armor are generally small and less than 3 V.

B. Distribution of Switching Transient Voltages

In this section, the switching transient simulations are performed based on energization of unloaded circuit and short circuit faults. The WB model [22] is used in the following time-domain studies.

1) Energization on an Unloaded Circuit

The circuit breakers CB1B, CB2A and CB2B shown in Fig. 1 are opened initially. A non-symmetrical energization is applied to upper circuit, and it means that Phase A, B and C of CB1A are closed at $t = 1$ ms, 1.5 ms and 2 ms, respectively.

The core voltages at both ends of cable in upper circuit are illustrated in Fig. 8. The maximum voltages at sending and receiving ends of cores appear on Phase A, and reach to 561.2 kV and 692.7 kV respectively. Based on [23], the maximum switching withstand voltage of 500 kV cable is 1175 kV. Thus, the margin of insulation coordination is around 41%.

(a) Voltage at sending end

(b) Voltage at receiving end
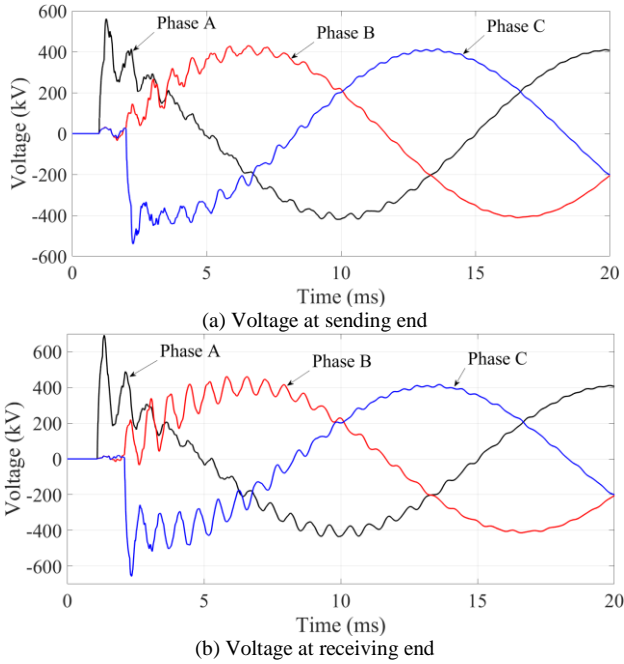
Fig. 8 Core voltage at both ends of cable in upper circuit.

The waveforms of transient sheath voltage at both ends of cable in upper and lower circuits are shown in Fig. 9. The maximum sheath and armor voltages of Phase A along the cable circuits are illustrated in Fig. 10. It should be noted that 200 random energizations have been performed to find the maximum overvoltages considering a stochastic behavior of breaker pole closing. The maximum voltages of energized circuit are higher than the results on the induced circuit. The sheath and armor voltage distributions of induced circuit are quite stable between 2 km and 16 km, and the maximum voltage is closed to 8 kV.

(a) Sheath voltage of cable in upper circuit

(b) Sheath voltage of cable in lower circuit
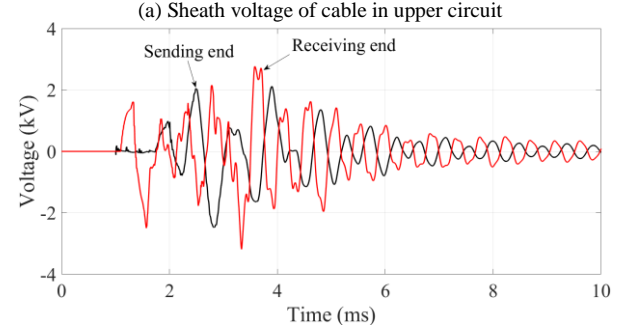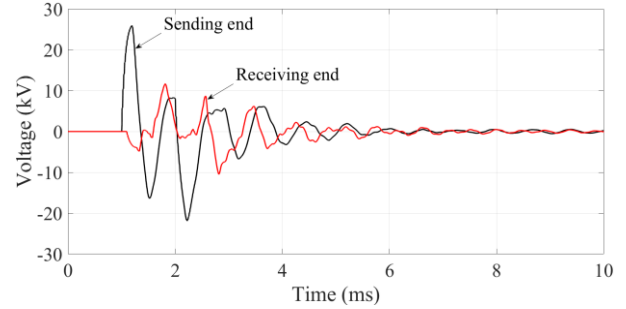
Fig. 9 Sheath voltage at both ends of cable in upper and lower circuits.
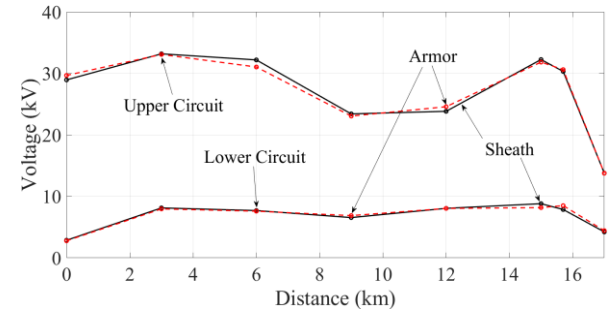
Fig. 10 Distribution of maximum transient overvoltage on sheath and armor of cable in upper and lower circuits, Phase A.

2) Short Circuit Fault

Both cable circuits illustrated in Fig. 1 are working in steady-state. Different short circuit faults are applied to the receiving end of overhead line 1 in the upper circuit through a fault resistance of 1 Ω. The various faults occur at $t = 0.1$ s, and then they are cleared by CB1A and CB1B with a time delay of 0.07 s.

The core voltages at receiving end of cable in upper and lower circuits are shown in Fig. 11 with consideration of a three-phase to ground fault. The maximum core voltage appears on Phase B with -491.5 kV.
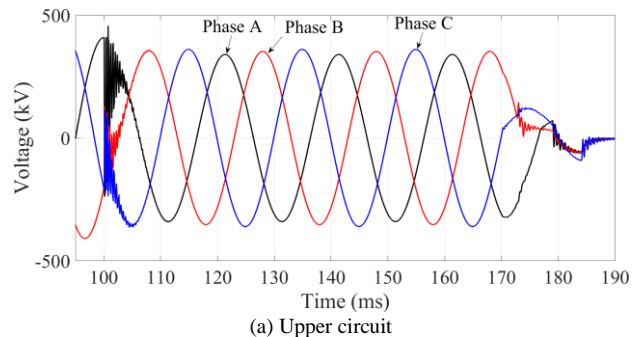
(a) Upper circuit
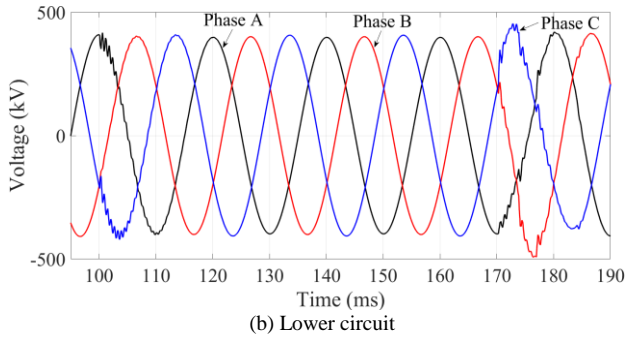
(b) Lower circuit

Fig. 11 Core voltage at receiving end of cable in upper and lower circuits, three-phase to ground fault.

The current of grounding resistance at sending end of cable in upper and lower circuits are illustrated in Fig. 12. It presents the general characteristics of currents in sheath and armor during the three-phase to ground fault. The clearance of the fault produces peak values of current in sheath and armor of cable, i.e. 7.12 kA and 3.72 kA for upper and lower circuits respectively.
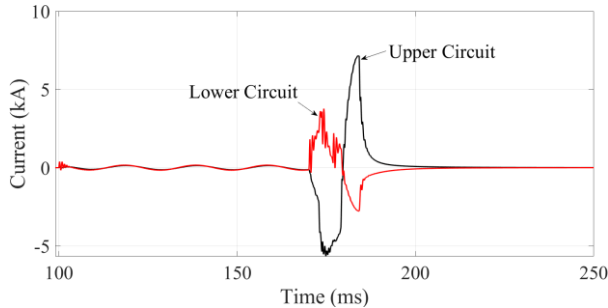
Fig. 12 Current of grounding resistance at sending end of cable in upper and lower circuits, three-phase to ground fault.

Fig. 13 shows maximum sheath and armor voltages in upper and lower cable circuits under different short-circuit cases. The voltages of sheath and armor on Phase A of cable are calculated. In general, the transient voltages on sheath are higher than the results of armor. The maximum voltage occurs on sheath in upper circuit at the distance of 3 km, and it reaches to 34.5 kV.
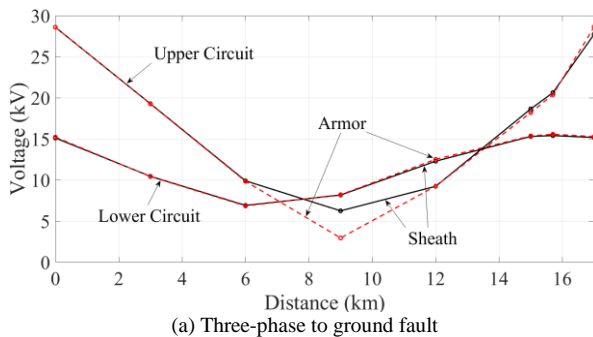
(a) Three-phase to ground fault
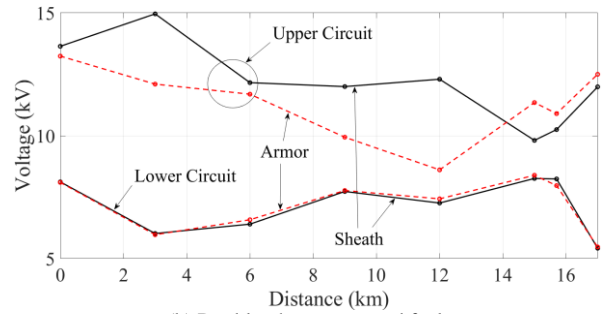
(b) Double-phase to ground fault
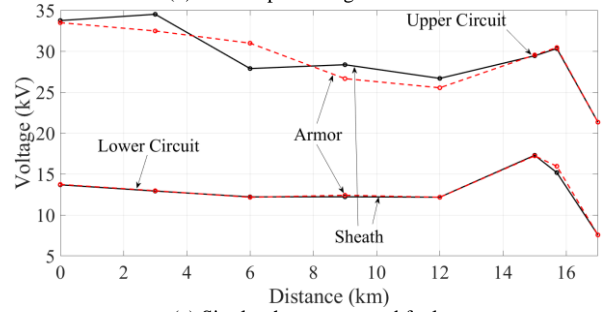
(c) Single-phase to ground fault

Fig. 13 Distribution of maximum transient overvoltage on sheath and armor of cable in upper and lower circuits with consideration of different faults, Phase A.

For unbalanced faults i.e. single-phase and double-phase to ground faults, the maximum transient voltages on sheath concentrates at the sending end of the cable in upper circuit. However, the transient voltages on sheath and armor excited by the symmetrical fault show the maximum level at both ends in the cable.

C. Distribution of Lightning Transient Voltages

According to report on lightning measurement in local region, the average strength of lightning is around 51.2 kA, the 13% of lightning current in whole year is larger than 80 kA [23]. The strongest lighting current appears in October each year, the average value is round 100 kA, and it maximally reaches 105 kA [23].

Therefore, the following study adopts a standard lightning impulse with current amplitude of 100 kA and wave front time of 1.2 μs/50 μs. The high frequency lumped grounding circuit shown in Fig. 6 has been used.

The lightning current flows into Phase A at receiving end of Overhead Line 1 in the upper circuit. The core voltages at receiving end of cable in upper and lower circuits are shown in Fig. 14. It should be noted that the maximum core voltage on Phase A in the upper circuit is 965.1 kV, and it becomes stable after 3 ms. Moreover, the maximum induced core voltage in the lower circuit appears on Phase C with -535.6 kV. The core transient overvoltages are lower than 1550 kV which is required by maximum lightning withstand voltage of 500 kV cable [23]. The margin of insulation coordination is around 37.7%.

(a) Upper circuit
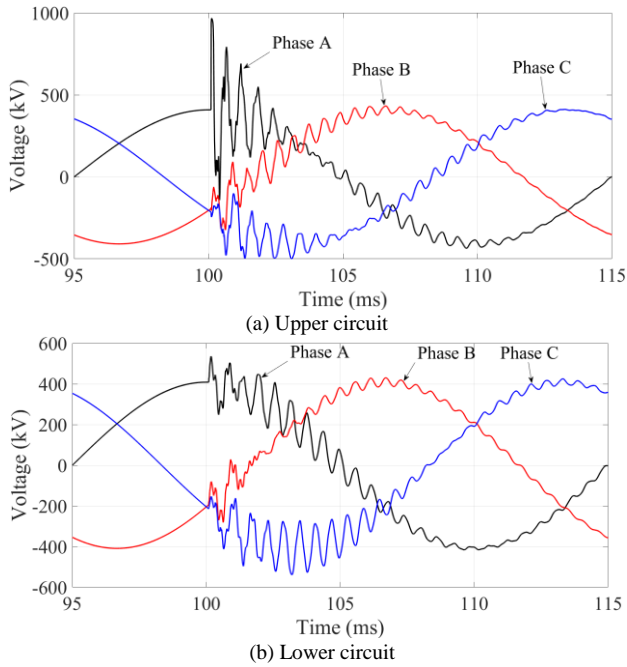
(b) Lower circuit

Fig. 14 Core voltage on receiving end of cable in upper and lower circuits.

The lightning induced currents flow through four grounding circuits shown in Fig. 1 are illustrated in Fig. 15. The maximum values occur in the energized circuit, and I_{g1} and I_{g2} are 13.1 kA and -10.7 kA respectively.
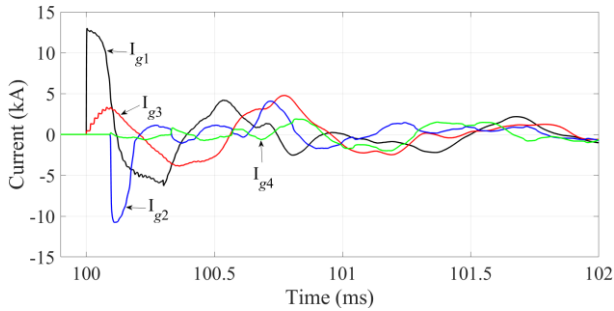
Fig. 15 Lightning current in grounding circuit.

The sheath voltages at both ends of the cable in upper and lower circuits with lightning strikes are shown in Fig. 16. The maximum voltage occurs at the sending end of the energized cable, and it reaches to 69.5 kV. The voltage on induced circuit is much lower, and it is 19.1 kV.
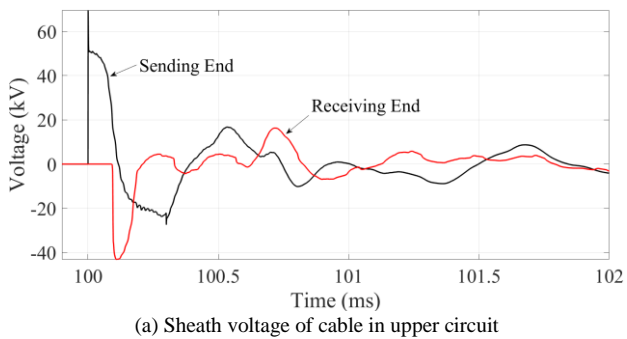
(a) Sheath voltage of cable in upper circuit
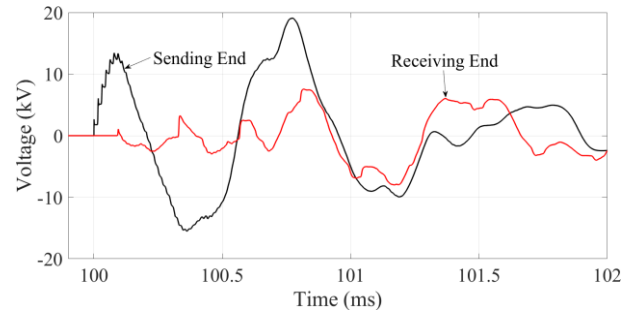
(b) Sheath voltage of cable in lower circuit

Fig. 16 Sheath voltage at both ends of cable in upper and lower circuits.

The distribution of maximum transient overvoltage between core and sheath of cable in upper and lower circuits is shown in Fig. 17. A transition between submarine cable to underground cable appears at 15.7 km, and the discontinuity of cable surge impedance causes a peak value around 16 km of the cable.
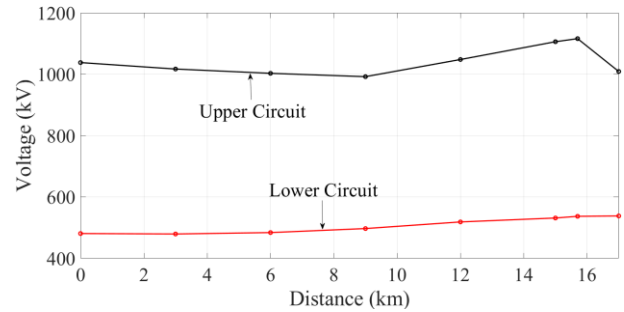
Fig. 17 Distribution of maximum transient overvoltage between core and sheath of cable in upper and lower circuits, Phase A.

Fig. 18 shows maximum sheath and armor voltages in upper and lower circuits by lightning strike. Again, the voltages of sheath and armor on Phase A of cable are recorded. It is clear that voltage decreases as distance increases. The voltages of sheath and armor on induced phase are 19.1 kV.
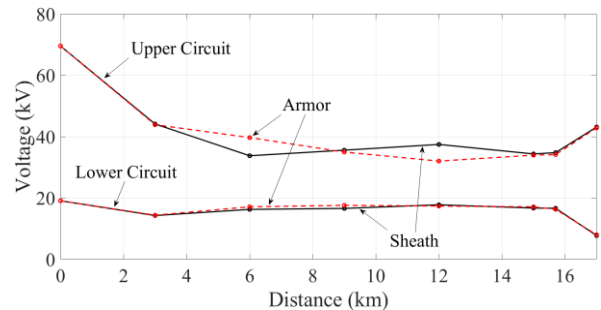
Fig. 18 Distribution of maximum transient overvoltage on sheath and armor of cable in upper and lower circuits, Phase A.

V. CONCLUSIONS

This paper performs frequency domain and time-domain studies on a 500 kV submarine cable which is a key part of a mixed transmission system. The results are obtained using an EMT-type simulation tool (EMTP). It has the following general conclusions.

· A practical 500 kV mixed transmission system has been introduced. The system consists of overhead lines,

submarine and underground cables.

- The series and shunt parameters of cable are calculated using recently developed new LCD module in EMTP. The wideband model has been adopted into the transient simulations of the system.

- The series impedance and modal propagation constants are evaluated with consideration of air, seawater and seabed structures. No instable characteristics are observed for calculated results.

- In the steady-state, the maximum induced sheath voltage of Phase A for cable in upper circuit appears at 9 km and reaches 80.1 V. Furthermore, the induced voltages on the same phase armor are generally small and less than 3 V.

- The maximum core voltages at sending and receiving ends for cable with energization of no-load occur at Phase A, and the voltages are 561.2 kV and 692.7 kV. The maximum sheath voltage appears at 6 km for energized circuit, and at 15 km for induced circuit.

- The transient voltages on sheath and armor excited by the symmetrical fault show the maximum level at both ends of the cable.

- The maximum core voltage at Phase A in the upper circuit is 965.1 kV for lightning transient. The maximum sheath voltage reaches to 69.5 kV.

- In general, the overvoltages of core, sheath and armor produced by different transient conditions are within the limit of insulation coordination regarding to references [24], [25].

- The investigations in this paper contribute to further understanding of cable insulation coordination in a mixed transmission system with accurate calculations of per-unit-length parameters.

VI. REFERENCES

[1] A. Ametani, H. Xue, T. Ohno and H. Khalilnezhad, *Electromagnetic Transients in Large HV Cable Networks: Modeling and Calculations*. London: IET Press, 2021.

[2] H. Khalilnezhad, M. Popov, L. van der Sluis, J. A. Bos and A. Ametani, "Statistical analysis of energization overvoltages in EHV hybrid OHL–Cable Systems," *IEEE Trans. Power Del*, vol. 33, no. 6, pp. 2765-2775, 2018.

[3] T. Henriksen, B. Gustavsen, G.Balog and U. Baur, "Maximum lightning overvoltage along a cable protected by surge arresters," *IEEE Trans. Power Delivery*, vol. 20, no. 2, pp. 859-866, 2005.

[4] L. Colla, F. M. Gatta, A. Geri and S. Lauria, "Lightning overvoltages in HV-EHV "mixed" overhead-cable lines," *International Conference on Power System Transients* (IPST), Lyon, 2007.

[5] F. Faria da Silva, K. S. Pedersen and C. L. Bak, "Lightning in hybrid cable-overhead lines and consequent transient overvoltages," *International Conference on Power System Transients* (IPST), Seoul, 2017.

[6] H. Xue, J. Mahseredjian, J. Morales, I. Kocar and A. Xemard, "An investigation of electromagnetic transients for a mixed transmission system with overhead lines and buried cables," *IEEE Trans. Power Delivery*, vol. 37, no.6, pp. 4582-4592, 2022.

[7] A. Ametani (editors), *Numerical Analysis of Power System Transients and Dynamics*, IET, 2015.

[8] A. Ametani, T. Ohno and N. Nagaoka, *Cable System Transients: Theory, Modeling and Simulation*, Wiley-IEEE Press, 2015.

[9] H.W. Dommel, *Line Constants*, Bonneville Power Administration, 1972.

[10] A. Ametani, *Cable Constants*, Bonneville Power Administration, 1976.

[11] A. Ametani, "A general formulation of impedance and admittance of cables," *IEEE Trans. PAS*, vol. PAS-99, pp. 902-910, 1980.

[12] H. Xue, A. Ametani, J. Mahseredjian and I. Kocar, "Computation of overhead line / underground cable parameters with improved MoM - SO method," *Power Systems Computation Conference* (PSCC), Dublin, 2018.

[13] H. Xue, A. Ametani, J. Mahseredjian and I. Kocar, "Generalized formulation of earth-return impedance / admittance and surge analysis on underground cables," *IEEE Trans. Power Delivery*, vol. 33, no.6, pp.2654-2663, 2018.

[14] H. Xue, A. Ametani, J. Mahseredjian, Y. Baba, F. Rachidi and I. Kocar, "Transient responses of overhead cables due to mode transition in high frequencies", *IEEE Trans. Electromag. Compat*, vol. 60, no. 3, pp.785-794, 2018.

[15] H. Xue, A. Ametani, J. Mahseredjian, Y. Baba and F. Rachidi, "Frequency response of electric and magnetic fields of overhead conductors with particular reference to axial electric field," *IEEE Trans. Electromag. Compat*, vol. 60, no. 6, pp. 2029-2032, 2018.

[16] H. Xue, A. Ametani and K. Yamamoto, "Theoretical and NEC calculations of electromagnetic fields generated from a multi-phase underground cable," *IEEE Trans. Power Delivery*, vol. 36, no.3, pp.1270-1280, 2021.

[17] H. Xue, J. Mahseredjian, J. Morales Rodriguez and I. Kocar, "Analysis of cross-bonded cables using accurate model parameters," *IEEE Trans. Power Delivery*, DOI: 10.1109/TPWRD.2022.3179832.

[18] H. Xue, J. Mahseredjian, A. Ametani, J. Morales and I. Kocar, "Generalized formulation and surge analysis on overhead lines: impedance/admittance of a multi-layer earth," *IEEE Trans. Power Delivery*, vol. 36, no. 6, pp. 3834-3845, 2021.

[19] H. Xue, A. Ametani and K. Yamamoto, "A study on external electromagnetic characteristics of underground cables with consideration of terminations," *IEEE Trans. Power Delivery*, vol. 36, no. 5, pp. 3255-3265, 2021.

[20] R. Alipio, H. Xue and A. Ametani, "An accurate analysis of lightning overvoltages in mixed overhead-cable lines," *Electric Power Systems Research*, vol. 194, 2021.

[21] J. Mahseredjian, S. Dennetière, L. Dubé, B. Khodabakhchian and L. Gérin-Lajoie, "On a new approach for the simulation of transients in power systems," *Electric Power Systems Research*, vol. 77, no.11, pp. 1514-1520, 2007.

[22] I. Kocar and J. Mahseredjian, "Accurate frequency dependent cable model for electromagnetic transients," *IEEE Trans. Power Del*, vol. 31, pp.1281-1288, 2016.

[23] Z. Zhou, X. Liu, S. Wang, C. Zhu, H. Liu and C. Song, "Simulation calculation of transient voltages on insulation and sheath along 500 kV XLPE submarine cable", *High Voltage Engineering*, vol. 44, no. 8, pp. 2725-2731, 2018.

[24] IEC, *Electric Cables - Tests on Extruded Oversheaths with A Special Protective Function*, IEC 60229:2007, 2017.

[25] IEEJ, Anti - Corrosion Layer for Power Cables, JEC 3402, 2001.